Journal of Thermal Analysis and Calorimetry, Vol. 64 (2001) 887–894

THE DETERMINATION OF DYNAMIC AND EQULIBRIUM SOLID/LIQUID TRANSFORMATION DATA FOR Sn–Pb USING DSC

A. S. Pedersen, N. Pryds, S. Linderoth, P. H. Larsen and J. Kjøller

Materials Research Department, Risø National Laboratory, DK-4000 Roskilde, Denmark

Abstract

Differential Scanning Calorimetric measurements were performed for accurate determination of the solidus and liquidus temperature of Sn–Pb alloys. The difference between onset and end temperature of the melting peak depended clearly on alloy composition. The results obtained were found to be in good agreement with the existing equilibrium phase diagram for the Sn–Pb system, although the data suggested a slight correction of the eutectic composition. Under cooling conditions a large variation in the onset temperature for solidification was found. A large number of heating and cooling cycles were performed in order to investigate the statistical variation of the solid nucleation process.

Keywords: DSC, equilibrium, melting, Sn–Pb alloys, solidification, undercooling

Introduction

Differential scanning calorimetry (DSC) is frequently used to determine the melting and solidification characteristics of metal alloys, e.g. melting temperature, enthalpy of fusion and onset temperature of phase transformation. Furthermore, in metallurgy the calculation and prediction of new phase equilibria requires a deep knowledge of the thermodynamic quantities such as Gibbs free energy of the phases and the involved elements expressed as a function of temperature [1]. The DSC instrument in this case provides an excellent way of obtaining such knowledge.

Various methods have been suggested in the literature for the determination of the melting curves of an alloy system using DSC [2–5]. However, only relatively few studies have been reported for the determination of crystallization data during cooling [6, 7]. This is probably due to the fact that calibration of the DSC equipment for cooling conditions is somewhat problematic because of the nucleation effect prior to solidification [7]. Nucleation is a problem of significant theoretical and practical interest. To some extent any liquid is undercooled before nucleation initiates the solidification, and the magnitude of the undercooling is an important parameter, which determines the development of microstructure, and hence the mechanical properties of the resulting material.

Sn–Pb alloys are widely used as a solder material in the electronic industry because of a low melting temperature, especially for the eutectic composition [8]. How-

1418–2874/2001/ $ 5.00

Akadémiai Kiadó, Budapest
Kluwer Academic Publishers, Dordrecht

ever there seems to be some variation in the values of the eutectic compositions reported in the literature. Thus the Sn–37 mass%Pb and the Sn–38 mass%Pb compositions are both reported to melt eutectically at 183°C [9, 10].

In the present study the DSC technique is used to investigate the melting and solidification of a series of Sn–Pb alloys (Pb< 40 mass%). Special attention is paid to the determination of the eutectic composition and melting temperature of this alloy. The solid nucleation process plays a decisive role for the undercooling prior to solidification. To study the nucleation phenomenon more closely we performed DSC measurements of several hundred heating and cooling cycles and examined the statistical variation of the nucleation temperature. This large number of data allows an investigation of the stochastic nature of the nucleation process [11]. The results of this investigation are discussed in the paper.

Experimental procedure

The samples of the investigated alloys were prepared from high purity elements (Pb 99.9999% and Sn 99.999%). Proper amounts of the materials were weighed with a precision of 0.1 mg and melted under vacuum in quartz tube while thoroughly stirred to ensure homogenisation. The prepared alloy compositions were Sn–10 mass%Pb, Sn–20 mass%Pb, Sn–36 mass%Pb, Sn–37 mass%Pb and Sn–38 mass%Pb (eutectic composition).

Differential scanning calorimetry (DSC) was carried out using a high sensitivity differential scanning calorimeter Seiko SII-DSC120 and a Seiko SII-DSC320. The samples (approx. 5 mg) were placed in aluminium pans with a mass of about 16 mg. During all the experiments a protection gas of pure He (99.996 %) was used with flow rate of 100 cm^3 min^{-1}. The DSC equipments are regularly temperature calibrated to within 0.5°C using melting of relevant metals.

The experiments were carried out for each alloy at different heating and cooling rates in the interval of 0.1–30°C min^{-1}. For the melting peaks two temperatures (the onset and the end temperature, which were identified by extrapolation) were determined as a function of heating rate. Extrapolation of these data to zero heating rate then yielded the equilibrium solidus and liquidus temperatures of the alloys. The onset (T_{mo}) and the end (T_{me}) temperature for the endothermic peak are identified as the solidus and the liquidus temperatures of the alloy respectively. As for the determination of the crystallization temperature the sample was cycled repeatedly between 120°C and 210°C at a rate of 10°C min^{-1} 360 times over a time period of 20 days.

Results and discussions

Melting

The dependence of the onset melting temperature on the heating rate was measured for different alloy compositions. For non-eutectic compositions the melting peaks at slow heating rates showed a splitting into two distinct peaks due to the sample's con-

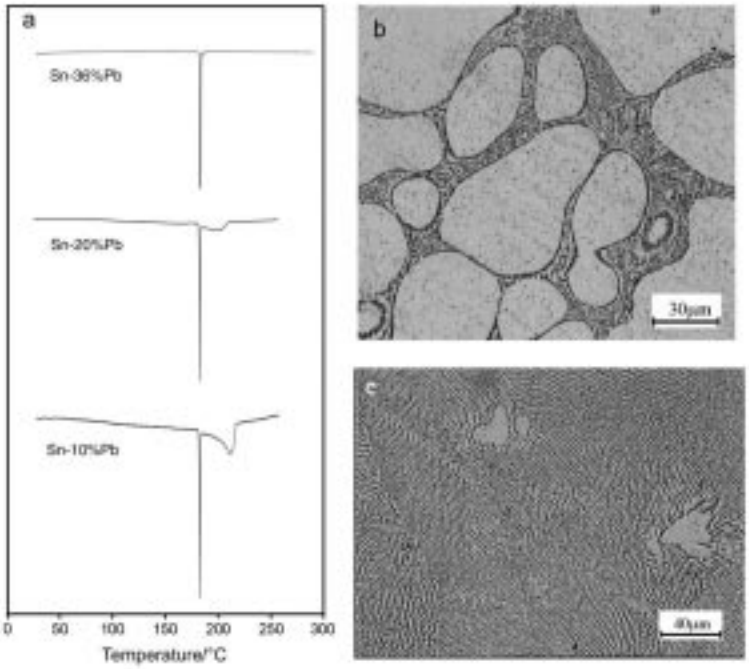

Fig. 1 Melting peaks of different compositions at heating rate 3°C min^{-1} (a). Micrograph of Sn–10% Pb showing large amount of β-Sn and only small amount of eutectic structure (b). Micrograph of Sn–36% Pb showing large amount of eutectic structure and almost no β-Sn (c)

tent of both Pb solid solution in Sn (β-Sn) and eutectic structure. Figures 1 a–c show the DSC melting results for different compositions at heating rate 3°C min^{-1} (a) and the corresponding microstructures (band c). The micrographs shown in Fig. 1 give a qualitative and quantitative illustration of the phase distribution for two different compositions (10 and 36% Pb). Inspection of Figs 1 b and c show, that the fraction of β-Sn is larger in the 10% than in the 36% Pb composition, and this is also reflected by the corresponding peak areas shown in Fig. 1 a. These observations are in accordance with the prediction of the well-known Lever Rule for phase distribution.

Figure 2 shows the onset and the end temperatures of the melting process for Sn–*n*Pb (*n*=10, 20, 36, 37 and 38.1 mass%) as a function of heating rate. The onset temperature was found to be independent of alloy composition and heating rate, whereas the end temperature depended linearly on heating rate with the same positive slope for all alloy compositions. A best linear fit to the onset temperature (T_{mo}) data yielded T_{mo}=(181.8±0.1)+(0.01±0.007)β, where β is the heating rate (°C min^{-1}).

Best linear fits to the end temperatures of the melting peaks as a function of heating rate yielded the following sets of equations,

Sn–10 mass%Pb	$T_{me}=(216.5\pm0.7)+(0.17\pm0.05)\beta$
Sn–20 mass%Pb	$T_{me}=(206.0\pm0.6)+(0.18\pm0.05)\beta$
Sn–36 mass%Pb	$T_{me}=(187.2\pm0.2)+(0.16\pm0.01)\beta$
Sn–37 mass%Pb	$T_{me}=(182.9\pm0.3)+(0.19\pm0.01)\beta$
Sn–38.1 mass%Pb	$T_{me}=(184.5\pm0.8)+(0.18\pm0.02)\beta$

again β is the heating rate (°C min^{-1}).

The slopes of these lines (Fig. 2) vary weakly depending on the alloy composition with an average of 0.18±0.07. Thus the general equation for the end melting temperature of Sn–*n*Pb at different heating rates can then be written as, $T_{me}=T_{me}^{0}+0.18\pm0.07\beta$, where T_{me}^{0} is the equilibrium end melting temperature, i.e. the liquidus point of the alloy, which is determined by extrapolating the data shown in Fig. 2 for different heating rates to zero heating rate. Figure 3 shows the end melting temperatures at zero heating rate for different alloy compositions.

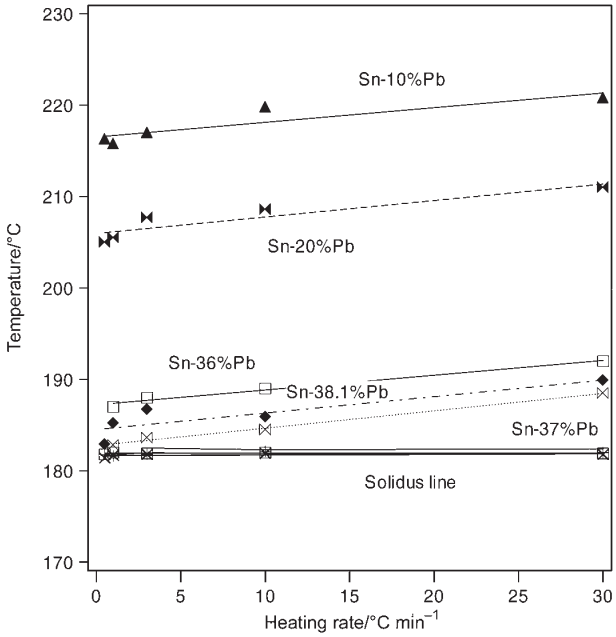

Fig. 2 The effect of heating rate on the onset and the end temperature of the melting peak for Sn–*n*Pb (*n*=10, 20, 36, 37 and 38.1 mass%) alloys. The symbols are the measured data points while the lines are linear fits to these data points

As seen from Fig. 3 up to a composition of about Sn–37 mass% Pb the liquidus line is characterised by a relatively steep negative slope. Above this Pb concentration the end melting temperature seems to increase, as indicated by the composition Sn–38.1 mass%Pb. In other words, the eutectic composition in which the slope changes from positive to negative lies in-between these two compositions and the eutectic temperature observed in this work is almost invariably 181.8°C.

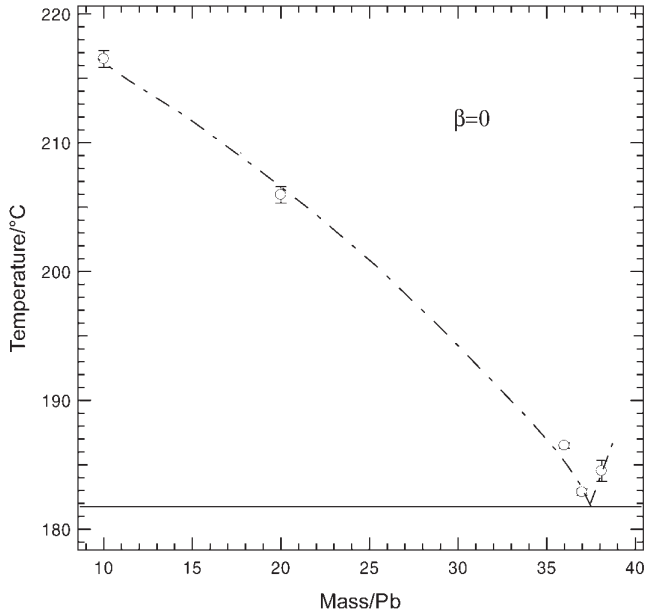

Fig. 3 The end melting temperature at zero heating rate for different alloy compositions. The horizontal line, ~181.8°C, represents the onset melting temperature of the alloy while the line with the negative slope represents the end temperatures of the melting peaks. The two lines thus correspond to the solidus and the liquidus lines (respectively) of the equilibrium phase diagram

A comparison of the present experimental data with the equilibrium data found in the Sn–Pb phase diagram from literature [9, 10] suggest a slight correction of the eutectic temperature and composition for the Sn–Pb system.

Solidification

The onset temperatures for the solidification, (i.e. the nucleation temperatures) of the Sn–Pb alloys were measured for the series of compositions described above. In the initial measurements, however, we observed a large variation in the results and it was not possible to correlate the obtained nucleation temperatures with neither sample size, cooling rate or any other recognisable, experimental parameters.

In order to study the variation of the nucleation temperature (undercooling), we performed a series of successive nucleation events by cycling the same sample (5.49 mg) of composition Sn–37%Pb in the DSC equipment 360 times using the same cooling rate in all cycles. Figure 4 shows the measured undercooling as a function of cycle number. It is seen from the figure, that during the first 30 cycles an almost linear increase in undercooling from approx. 15 to 33°C was found and after that the nucleation temperatures seemed to be more or less constant scattering around an undercooling of 33°C. Figure 5 shows the distribution function for the observed

undercooling temperatures represented in a bar diagram. If the first 25 cycles are disregarded the average undercooling temperature is 32°C and the variance is 2.7°C.

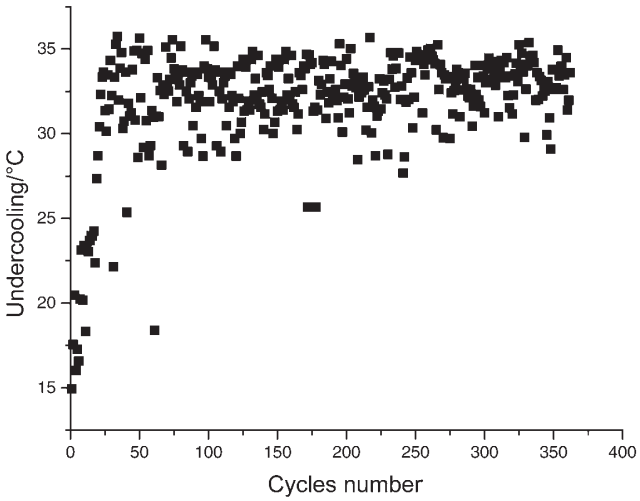

Fig. 4 Undercooling values of Sn–37%Pb measured successively by cycling the sample between 120 and 210°C using the same cooling rate in all cycles

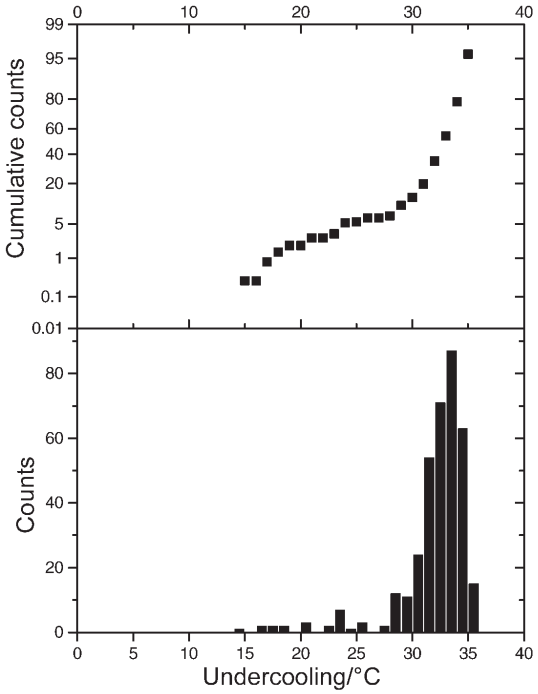

Fig. 5 Distribution functions for measured undercooling for 5.49 mg of Sn–37%Pb

Other workers have found the same kind of scatter, as described above, in results of similar experiments using pure Au and Al. For gold Wilde *et al.* [11] found a linearly increasing undercooling from zero to 200°C over the first 25 cycles. In the following range up to 600 cycles the undercooling values scattered around 212°C with an approximate standard deviation of 5°C. For aluminium Perpezko *et al.* [12] found a considerably smaller scatter and no initial change in the value of undercooling.

The reason for the initial increase in undercooling seen in Fig. 4 is not clear. However, the increase indicates the absence of catalytic nucleation sites. It has been suggested [12], that nucleation sites in the form of impurity clusters or particles are segregated or rendered inactive during the initial cycles. The authors do not give an explanation as to which mechanisms could give rise to such processes. We suggest, that during solidification of the Sn–Pb alloy the progressing solid/liquid interface expels impurity atoms into the liquid phase and by that process the impurity atoms are transported to the surface. At the surface the impurities are not any longer active as a bulk nucleation site because they either evaporate from the surafce, react with the atmosphere or just remain in the form of clusters on the surface of the sample. The process is not completely effective, but over a number of solidifications, which in our case seems to be approximately 25 (Fig. 4), the majority of impurities have been concentrated at the sample surface. At this stage the undercooling becomes constant with time (Fig. 4). Evidence for the impurity effect on the undercooling has been observed [11, 13] when we compared the results of gold (Au) samples with different purities which were subjected to a large number of cycles. In that case, the undercooling was observed to stabilise at a higher undercooling value and a shorter increasing linear stage for the sample with high purity. Currently we are doing further experimental work aiming to explain the systematic change of nucleation temperature during the first cycles.

Conclusions

The present work has shown, that accurate, thermodynamic equilibrium data can be extracted from dynamic DSC measurements. The data obtained for the melting of Sn–Pb alloys are largely in agreement with the existing phase diagram, but the results suggest a minor correction of the eutectic temperature and composition for the system.

Under cooling conditions a considerable variation was found for the solidification onset temperature (i.e. solid nucleation temperature). Extended measurements on a large number of nucleation events showed, that undercooling increased from 15 to 33°C during the first 25 solidifications and from that stage a stable undercooling was seen for the next 335 solidifications with a variance of 2.7°C. The change of the undercooling is explained tentatively in terms of sample purification as a result the repeated solidifications.

Finally, the present results indicate that in order to determine accurately the value of the undercooling the present statistical approach must be applied.

The authors wish to thank M.Sc. A. Dinesen for valuable assistance in the statistical analysis of the data for undercooling.

References

1 R. Ferro, G. Borzone, G. Cacciamani and Raggio, Thermochim. Acta, 347 (2000) 103.
2 S. M. Sarge, W. Hemminger, E. Gmelin, G. W. H. Höhne, H. K. Cammenga and W. Eysel, J. Thermal Anal., 49 (1997) 1125.
3 A. N. Sembira and J. G. Dunn, Thermochim. Acta, 274 (1996) 113.
4 J. A. Martins and J. J. C. Cruz-Pinto, Thermochim. Acta, 332 (1999) 179.
5 E. Gmelin and St. M. Sarge, Pure & Appl. Chem., 67 (1995) 1789.
6 G. Hakvoort and C. M. Hol, J. Therm. Anal. Cal., 52 (1998) 195.
7 G. Hakvoort and C. M. Hol, J. Therm. Anal. Cal., 56 (1999) 717.
8 R. J. Klein Wassink, Soldering in Electronic, 2nd ed., Electrochemical Publications, British Isles 1989.
9 S. W. Chen, C. C. Lin and C. M. Chen, Metall. Mater. Trans. A, 29A (1998) 1965.
10 T. B. Massaski, H. Okamoto, P. R. Subramanian and L. Kacprzak (eds.), Binary Alloy Phase Diagrams, Second Edition, ASM International, USA 1992, p. 3014–3017.
11 G. Wilde, J. Sebright, P. Höckel and J. Perepezko, Materials Development and Processing-Bulk Amorphous Materials, Undercooling and Powder Metallurgy, EUROMAT 99, Ed. J. V. Wood, L. Schultz and D. M. Herlach, Wiley-VCH 1999, p. 85–91.
12 J. H. Perepezko, J. L. Sebright, G. Wilde and P. G. Höckel, Intern. Conf. on Spray Deposition and Melt Atomization (SDMA 2000), Ed. K. Bauckhage, V. Uhlenwinkel and U. Fritsching, Bremen, Germany 2000, p. 613–626.
13 Data to be published.